

Cross-layer Balance of Visuo-hippocampal Functional Connectivity Is Associated With Episodic Memory Recognition Accuracy

Wei-Tang CHANG (✉ weitang_chang@med.unc.edu)

University of North Carolina at Chapel Hill

Stephanie Langella

Massachusetts General Hospital

Min Sung Seo

University of North Carolina at Chapel Hill

Khoi Huynh

University of North Carolina at Chapel Hill <https://orcid.org/0000-0001-9538-2408>

Pew-Thian Yap

University of North Carolina at Chapel Hill <https://orcid.org/0000-0003-1489-2102>

Weili Lin

University of North Carolina at Chapel Hill

Kelly Giovanello¹

University of North Carolina at Chapel Hill

Article

Keywords:

Posted Date: June 28th, 2022

DOI: <https://doi.org/10.21203/rs.3.rs-1789565/v1>

License:   This work is licensed under a Creative Commons Attribution 4.0 International License.

[Read Full License](#)

Abstract

Episodic memory is supported by the hippocampus and widespread cortical areas. However, little is known about how hippocampal subregions connect with different cortical layers or how layer-dependent cortico-hippocampal functional connectivity (FC) correlates with memory performance. Inspired by cross-frequency coupling between the hippocampus and neocortex in intracranial electrophysiological studies, we hypothesized that the balance of cortico-hippocampal FC strengths between deep and superficial layers would be associated with recognition memory accuracy. To test this hypothesis, we developed laminar-resolution fMRI, achieving whole-brain coverage, 1-mm isotropic resolution, and 2-second temporal resolution on a 7T scanner by integrating multiple advanced methods. Our results showed that the balance of cortico-hippocampal FC between superficial and deep layers in visual cortex was more highly correlated with recognition accuracy than conventional layer-averaged FC. Such findings open a new avenue for layer-dependent FC research, with clear implications for future investigations into clinical populations.

Introduction

The episodic memory system, which supports learning and remembering distinct events and associations among informational elements, plays an essential role in everyday life. Tremendous effort has been put forth to understand the underlying neural processes of this system¹. Patient studies of individuals with bilateral hippocampal lesions have revealed a critical role of the hippocampus for successful retrieval of associative memories², with supporting evidence from functional magnetic resonance imaging (fMRI) studies highlighting significant hippocampal activity during associative memory encoding and retrieval^{3–5}. The episodic memory system also engages multiple cortical areas, including the medial temporal lobe (MTL)^{6,7}, visual cortex (VC)^{8,9}, posterior parietal cortex (pPC)^{6,10}, lateral prefrontal cortex (IPFC)^{11,12}, and default-mode network^{13,14}.

Beyond such conventional fMRI investigations that identify regional changes in blood-oxygen-level-dependent (BOLD) activity, a growing body of research examines the interactions, or functional connectivity (FC), between the hippocampus and cortical regions^{15,16}. Widespread cortico-hippocampal FC supports both successful memory encoding and retrieval, with distinct connections supporting encoding versus retrieval along the long-axis of the hippocampus¹⁷. Consistent with findings of differential FC patterns across hippocampal subregions¹⁷, studies of hippocampal circuitry have revealed functional dissociations between anatomical subfields, e.g., *cornu ammonis* (CA) areas 1 through 4 and dentate gyrus (DG), and along the anterior-posterior gradient^{18,19}. These distinct subregions also differentially connect to nearby regions, such as parahippocampal cortex and striatum, during episodic memory tasks^{20,21}. However, little is known about subregional connectivity across cortex. Furthermore, most whole-brain fMRI studies utilize a spatial resolution of 2–4 mm, resulting in considerable partial volume effects when examining activity of hippocampal subfields that are as thin as ≤ 1 mm. Although some studies of hippocampal subfield function have utilized smaller voxel sizes (~ 1.5 mm)^{22,23}, the field

of view has been limited to the medial temporal lobes, thereby precluding analyses of cortico-hippocampal subfield BOLD activity and FC.

Similarly, little is known about functional dissociations among cortical layers. Recent primate studies suggest that superficial and deep cortical layers exhibit distinct neurophysiological characteristics. Cortical rhythms in the alpha/beta band are associated with deep layers, whereas gamma rhythms are associated with superficial layers^{24–26}. Beta- and gamma-band activities in humans have also been shown to be associated with deep and superficial cortical layers, respectively²⁷. However, human cortical thickness is approximately 2–4 mm²⁸, meaning in an fMRI investigation with typical voxel size, differences in the BOLD signal across varying cortical depths cannot be detected. Spatial resolution of at least 1 mm is necessary to tease apart both the hippocampal subregions, as well as the deep and superficial cortical layers.

Based on the limited number of intracranial electroencephalogram (EEG) studies, recognition accuracy is associated with the coupling between cortical alpha/beta/gamma amplitude and hippocampal theta/gamma band activity^{29,30}. Together with the depth-dependent EEG-BOLD association in humans²⁷, these findings led us to reason that the hippocampus is coupled with both the deep and superficial cortical layers during episodic memory. If such layer-specific cortico-hippocampal couplings may be detected by fMRI, the strengths of cortico-hippocampal FC associated with deep and superficial layers are expected to be balanced during episodic memory encoding and retrieval. Balanced cortico-hippocampal FC strengths between deep and superficial layers imply that the FCs associated with both layers have similar strength.

Accordingly, we hypothesized that the balance of cortico-hippocampal FC strengths between deep and superficial layers would be correlated with recognition accuracy. Secondly, we hypothesized that the cross-layer balance of FC strengths would be more indicative of recognition accuracy than the layer-averaged cortico-hippocampal FC. Our hypotheses, if supported, would open a new avenue for fMRI FC research, as layer-dependent cortico-hippocampal FC is largely unexplored. Nevertheless, testing these hypotheses requires the technical challenge of achieving spatial resolution of at least 1 mm isotropic, temporal resolution of 2 s, and whole-brain coverage. Due to the technical limitations of imaging acceleration capability, however, current ultrahigh-resolution fMRI acquisitions compromise the ability to acquire either whole brain images³¹ or a high temporal resolution (< 3s)³². Moreover, the signal-to-noise ratio (SNR) is inherently low not only in accelerated images, but also in the reference scans. Insufficient SNR in the reference image compromises the quality of the reconstruction kernel and deteriorates the quality of reconstructed images.

To overcome these challenges, we incorporated several advanced methods into both fMRI acquisitions and reconstructions, including a multi-shot approach with the reference scan for SNR enhancement, blipped-Controlled Aliasing in Parallel Imaging (blipped-CAIPI) in the acceleration scan for the g-factor reduction³³, and the Marchenko-Pastur principal component analysis (MPPCA) method³⁴ in image reconstruction for the thermal-noise suppression. Taken together, we achieved laminar-resolution fMRI

with whole-brain coverage, 1-mm isotropic resolution, and volumetric scan time of 2 s on a 7T scanner. An associative memory task was designed to elicit hippocampal and cortical activity. We first analyzed the event-related BOLD responses and then defined the cortical and hippocampal regions of interest (ROIs) accordingly. Based on those ROIs, we examined the layer-dependent cortico-hippocampal FC during encoding and retrieval stages and its association with retrieval performance. The balance of cortico-hippocampal FC between superficial and deep layers in visual cortex demonstrated a stronger correlation with recognition accuracy than the conventional layer-averaged cortico-hippocampal FC, thereby supporting future investigation on layer-dependent FC.

Results

Task description

Participants completed six alternating encoding and retrieval phases of an associative memory task within the scanner (see Fig. 1). During encoding, participants studied pairs of names of famous figures and pictures of everyday objects. Participants were instructed to think of the person interacting with the object. Immediately following encoding, participants completed the retrieval phase, during which participants responded whether a presented name-object pair was the same or different from what they studied at encoding.

Layer-dependent and hippocampal evoked BOLD responses

The activation maps, reflecting evoked BOLD responses on the cortical surface averaged across cortical depths, during memory encoding and retrieval are shown in Fig. 2a. The visual cortex (VC), posterior parietal cortex (pPC), and dorsal lateral prefrontal cortex (dlPFC) had positive BOLD responses in both encoding and retrieval stages, whereas the medial prefrontal cortex (mPFC) had negative BOLD deactivations during the retrieval stage, as reported in prior episodic memory studies^{35,36}. In general, the cortical activation pattern during encoding was similar to that during retrieval, which is consistent with the principle of transfer-appropriate processing (TAP) that memory retrieval involves the reinstatement of processes active at the time of encoding³⁷. We further investigated the cortical-depth profile in the functionally-defined cortical ROIs (highlighted in yellow in Fig. 2b). The BOLD signal changes in VC and dlPFC across cortical depths in the encoding stage were statistically similar to that in the retrieval stage. Significant differences between memory stages were observed for the mPFC ROI, especially in the deep layers (uncorrected $p < 0.001$), and for the pPC ROI (uncorrected $p < 0.05$).

The hippocampal activation maps of both memory stages are depicted in Fig. 2c. We merged the two maps and identified the largest two clusters for the subsequent FC analysis (Fig. 2d). One cluster is in the anterior hippocampus, and 63% of the cluster is CA4/DG which is associated with pattern separation^{38,39}. The other cluster is in the posterior hippocampus, and 50% of the cluster is presubiculum which receives direct visual information from primary and secondary visual cortices⁴⁰.

Layer-dependent cortico-hippocampal FC

Using the functionally-defined hippocampal seeds (see Fig. 2d), the cortical-depth profiles of cortico-hippocampal FC were computed (see Fig. 3). Significant differences in FC strength between encoding and retrieval stages were observed between the aHP seed and VC and pPC. Conversely, significant differences in FC strength between mnemonic stages were observed between the pHP seed and the pPC and mPFC ($p < 0.05$). Note that the mnemonic stage differences in VC were not significant for BOLD signal changes but were for aHP-associated FC strength, suggesting the BOLD activation and BOLD FC provide complementary information. This is in line with the early human and primate studies that indicate BOLD activation is more associated with gamma activities, whereas the BOLD FC is predominantly contributed by low-frequency oscillations^{41,42}.

Behavioral correlates with cortico-hippocampal FC

To test whether the imbalance of cortico-hippocampal FC between deep and superficial layers is indicative of recognition accuracy, regression analyses were performed on all hippocampal seed and cortical ROI pairs. Figure 4a shows the scatter plots and associated regression lines for all pairs during memory encoding. The pHP-VC was the only pair that was significantly correlated with recognition accuracy (uncorrected $p < 0.01$; FDR corrected $p = 0.055$). During retrieval, the aHP-VC was the only pair that was significantly correlated with recognition accuracy (uncorrected $p < 0.001$; FDR corrected $p < 0.01$). Thus, in both encoding and retrieval stages, the VC was the only cortical region that was indicative of behavioral performance.

To further understand whether the cross-layer imbalance is the best predictor compared to other FC measures, we also performed behavioral correlations with the FC associated with (1) all layers averaged, (2) deep layers only, and (3) superficial layers only. Because VC was the only cortical connection which was significantly associated with accuracy, hippocampal seed – VC FC was the focus of this analysis. Statistical comparisons of the regression lines between the predictors were conducted using the bootstrapping method (number of iterations = 500) because the cross-layer imbalance of FC was not independent of other FC measures. For the aHP-VC FC during the retrieval stage, the imbalance of FC showed the highest R^2 with the bootstrap $p < 0.001$ compared to all other connections (Fig. 5a). Likewise, pHP-VC FC during the encoding stage was a significantly better predictor than other FCs ($p < 0.001$ using bootstrapping; Fig. 5b).

Discussion

Although animal studies have demonstrated that superficial and deep cortical layers exhibit different neural characteristics, corresponding studies in humans are scant due to the technical challenges of laminar imaging. In this study, we developed whole-brain fMRI with 1-mm isotropic resolution and TR of 2s, enabling the investigation of layer-dependent cortico-hippocampal FC. During the associative memory task, the evoked BOLD responses in visual cortex during encoding and retrieval stages were statistically

similar, replicating the principle of TAP³⁷. Nevertheless, FC with anterior hippocampal subregion (aHP) during encoding was significantly higher than during retrieval. Moreover, the cross-layer imbalance of visuo-hippocampal FC was significantly correlated with in-scanner recognition accuracy, such that higher imbalance was associated with lower recognition accuracy. Our results also showed that the cross-layer balance of visuo-hippocampal FC predicted recognition accuracy better than the conventional layer-averaged FC.

Although the memory task evoked activity in multiple cortical and hippocampal regions, we were particularly interested in understanding which subregions are most predictive of recognition accuracy. Recognition accuracy has been shown to be associated with the reactivation of lower-level image features within the visual cortex rather than high-level categorical features, particularly during tasks which require discriminating visual features⁴³. Results from the FC-behavioral correlations are consistent with those findings, showing significant behavioral correlates only in visual cortex.

The behavioral correlation demonstrated, for the first time, the relationship between the cross-layer imbalance of cortico-hippocampal FC and recognition accuracy. The neocortical and hippocampal oscillatory activities during episodic memory processing were demonstrated to be coupled according to the neural chronometry²⁹. Specifically, the desynchronization of neocortical alpha/beta oscillatory facilitated the processing of event-related information²⁹, while the synchronization of hippocampal theta/gamma oscillatory facilitated information binding^{44,45}. In addition, the deep and superficial layers were also coupled during memory processes in a way that the phase of deep-layer alpha/beta rhythms modulated the amplitude of superficial-layer gamma rhythms⁴⁶. Thus, hippocampal activity was coupled with both deep- and superficial-layer activities during memory processes. Assuming that neural coupling is detectable by fMRI-based FC, we hypothesized that a higher imbalance between hippocampal-deep layer and hippocampal-superficial layer FC strengths is associated with lower recognition accuracy. In general, our results of visuo-hippocampal FC, shown in Fig. 4, supported this hypothesis, demonstrating the hypothesized behavioral correlations during both encoding and retrieval stages.

Despite the significant behavioral correlations, however, the hippocampal subregions that were involved in the correlations were unexpected. As shown in Fig. 2d, the pHP exhibited higher BOLD activation than aHP during memory retrieval. Nevertheless, the hippocampal subregion that was involved in the significant behavioral correlation during retrieval was aHP rather than pHP (see Fig. 4b). Likewise, pHP exhibited weaker BOLD activation during encoding but was involved in the higher FC-behavioral correlation (see Fig. 4a). A potential explanation for these seemingly counterintuitive results centers on the neural basis of the event-related BOLD activation. A large body of evidence indicates that the BOLD signal is positively correlated with gamma activity^{42,47}. The positive hemodynamic responses generally follow the canonical model⁴⁸ which is commonly used in standard fMRI analyses⁴⁹. Thus, a brain region that is dominated by event-related gamma activity would be more “visible” in fMRI results. On the contrary, low-frequency activity (< 20 Hz), such as theta and alpha rhythms, is negatively correlated with the BOLD signal⁵⁰. If a brain region is not dominated by gamma activity but rather comprised of a

mixture of high- and low-frequency bands, the event-related BOLD response might be deviated from the canonical model and become less significant in the standard statistical results. Based on the finding that theta and gamma bands are the most prominent rhythms recorded in the hippocampus⁴⁵, we suspect that the neural activity in aHP during memory retrieval is predominantly in the theta band, which may explain the weak BOLD activation but the significant involvement in the behavioral correlation with recognition accuracy. Supporting this hypothesis, it has been previously demonstrated that the brain regions with strong theta rhythms were not in the proximity of fMRI activation⁵¹.

To test this hypothesis directly, however, electrophysiological and fMRI recordings in hippocampus are necessary. Since this study used fMRI only, EEG measurement should be included in future research to investigate the neural basis of the layer-dependent cortico-hippocampal FC. For example, intracranial EEG and fMRI measurements on epileptic patients or simultaneous recordings of scalp EEG and fMRI would help to elucidate the frequency-dependent EEG-fMRI relationship in hippocampus and neocortex. This article serves as an open call to the research community to explore the layer-dependent cortico-hippocampal FC – a new avenue to understand the mechanisms of the episodic memory process.

Despite the unprecedented features of our layer-dependent fMRI, this study has several limitations as follows. 1) Susceptibility effect: Due to the strong susceptibility effect on 7T scanners and relatively longer echo train in high-resolution fMRI, the inferior frontal and temporal lobes suffer from signal loss even after distortion correction. This study mitigated this issue by applying partial Fourier and changing the phase encoding (PE) direction from anterior-posterior to superior-inferior, which shortened the echo train by ~ 50%. The employment of in-plane acceleration also reduced the effective echo spacing and echo-train length, alleviating the susceptibility artifact. Even so, the signal loss in some of the highly susceptible regions was inevitable. This might explain the lack of significant activation in temporal lobe in this study which was previously reported during episodic memory tasks¹³. 2) Effective resolution: T2* decay along the EPI readout may lower the effective spatial resolution⁵². With the scan protocol in our study, however, the spatial blurring caused by T2* decay is calculated to be only ~ 8% (detailed in Supplementary materials)⁵³. Consistent with the theoretical calculation, the empirical results showed 9% increase of full-width-half-magnitude (FWHM) along PE direction compared to frequency encoding (FE) direction (see Figure S4). 3) Draining-vein effect: The BOLD signal towards superficial cortical layers is known to be confounded with unwanted venous signal due to the blood drainage via large veins⁵⁴. The draining-vein effect may add in task-irrelevant signal (offset model), amplify the layer-specific signal (scaling model), or cause the signal leakage from deep to superficial layers (leakage model)⁵⁵. Although several model-based corrections of draining-vein effect are available, none of them has been proven to be superior than the others. Without the standardized deveining process, we decided not to apply the deveining method in this study. While we do not expect the draining-vein effect is responsible for the observed behavioral correlation, it is worthwhile to evaluate to what extent the layer-dependent FC is affected in the future. 4) Head motion: The high-resolution fMRI is also more sensitive to head movement. To minimize the motion artefact, this study set the exclusion criteria that the dataset with the relative motion ≥ 1 mm will be excluded. However, none of the dataset was excluded by the criteria. The

absolute head displacement in this study is 0.05 mm in average and the maximal head displacement is 0.11 mm. 5) Generalization: Last but not least, it is unclear whether the findings in this study could be generalized to cognitive tasks other than the associative memory task employed in this study. Further studies are needed to test the hypothesis with other memory tasks and cognitive domains.

The discovered behavioral correlation with the cross-layer imbalance of cortico-hippocampal FC could have great impact outside of healthy young adults, particularly for examining biomarkers of neurodegenerative diseases. As deep/superficial cortical layers were associated with low/high-frequency oscillations, the high/low frequency power imbalance has been shown to be associated with early Alzheimer's disease⁵⁶. The alterations in hippocampal theta-gamma coupling were found to start earlier than plaque deposition⁵⁷. Cortico-hippocampal networks have also been found to be susceptible to normal and pathological ageing^{58,59}. The characterization of such a cross-layer difference has the potential to lay the fundamental step towards the development of a sensitive biomarker for pathological ageing. Furthermore, the neuronal oscillations at different frequencies were known to be associated with different neural circuits⁶⁰ and cell types. For example, the GABA neurons in the medial septum were engaged in generating hippocampal theta rhythms⁶¹. Therefore, our framework will also provide potential targets for early therapeutic intervention.

In sum, the results reported in this study provide a novel and exciting new direction for studying cross-layer imbalance in humans. We showed that cortico-hippocampal FC differs across cortical layers during mnemonic stages, and that cross-layer imbalance provides improved prediction of recognition accuracy compared to typical layer-averaged FC. Future investigations into layer-dependent cortico-hippocampal FC may provide important information into various clinical populations.

Methods

Participants

Twenty-four healthy young adults were recruited for this study. One participant was not able to complete the study due to physical discomfort. The datasets of two other participants were invalid due to the lack of reversed phase-encoding echo-planar imaging (EPI) for distortion correction. Data from twenty-one participants were included in the analysis (aged 20.7 ± 3.5 years, 8 males). Participants were screened to ensure they had no history of neurological or psychiatric conditions, previous head trauma, or MRI contraindications. Informed consent was obtained from each participant prior to the study in accordance with the experimental protocol approved by the University of North Carolina at Chapel Hill Institutional Review Board.

MR Acquisitions

MR images were acquired using a Siemens 7T Magnetom scanner (Siemens Healthcare, Erlangen, Germany). Two resting-state scans and 6 pairs of task scans were acquired using customized simultaneous multislice echo-planar imaging (SMS EPI) sequence. As the image reconstruction is

sensitive to the quality of the reference scan, multi-shot imaging was used in order to enhance the signal-to-noise ratio (SNR) (See Figure S1). The number of shots = 5. The spatial resolution was 1.0 mm isotropic using the following imaging parameters: FOV = 152×120×175 (R-L×H-F×A-P) mm³; number of coronal slices = 175; TE = 23 ms; number of partition encoding (PAE) = 5; TR per shot = 400 ms; effective TR = 2 s; effective SMS factor = 7; in-plane acceleration = 2; partial Fourier = 6/8. The EPI with opposite direction of phase encoding was also acquired for distortion correction. The number of image volumes for resting/encoding/retrieval scans was 180/117/74. The T1-weighted anatomical image with 1-mm isotropic resolution was acquired using Magnetization Prepared Rapid Gradient Echo (MPRAGE) image with the following parameters: TR/TE/TI = 2200/2.78/1050 ms, flip angle = 7°, partition thickness = 1 mm, image matrix = 256 × 240, 192 partitions, and FOV = 25.6 cm × 24 cm. The axial slab that encompassed the hippocampus was also acquired using ultrahigh-resolution Turbo spin-echo (TSE) image with 0.6 mm isotropic resolution.

Data Preprocessing

Before image reconstruction, the raw images of EPI were de-noised using the Marchenko-Pastur principal component analysis (MPPCA) method which has been shown to be effective in thermal noise removal³⁴ (See Figure S2). EPI time series were reconstructed using Generalized Autocalibrating Partial Parallel Acquisition (GRAPPA)⁶². Time-series data were motion corrected using FSL and then distortion corrected using FSL TOPUP⁶³. The corrected data were decomposed into a number of independent components by MELODIC⁶⁴. With the resting runs acquired from 15 participants, we trained the ICA-based denoising tool FIX to auto-classify ICA components into signal and noise components⁶⁵. The noise components were then removed by FIX using the threshold of 20. The time-series signals were band-pass filtered from 0.01 to 0.15 Hz. The individual T1 volume was coregistered linearly onto the time-averaged EPI volume using Advanced Normalization Tools (ANTs; <http://stnava.github.io/ANTs/>). With the decent coregistration quality (see Figure S3), the processed EPI volumes were resampled onto a cortical surface at different cortical depths using the freesurfer command 'mri_vol2surf'. According to the suggestion by LayNii that the number of layers may be set to at least 4 times larger than the resolution⁵⁵, we subdivided the cortex depth into 12 layers, assuming typical cortical thickness is 3 mm. Surface-based spatial smoothing was applied with full-width half-magnitude (FWHM) of 3 mm.

Task Stimuli and Design

Stimuli included 252 names of famous figures and 288 color pictures of everyday objects. Names were chosen for famous figures who are currently living and who are known by a first and last name. Pictures consisted of full color photographs of the object against a white background, collected from the Mnemonic Similarity Task⁶⁶. Names and pictures were separated into six equal lists of 42 names and 48 pictures each, and no first or last name overlapped within a list. Within each list, pictures were counterbalanced for stimulus condition, and names were randomly paired with images.

Both encoding and retrieval phases were scanned, and encoding and retrieval runs alternated for a total of six testing blocks. Each trial began with a fixation cross of variable interstimulus interval, determined

using OptSeq⁶⁷ (range: 0ms to 6000ms; average duration: 1000ms). At encoding, 42 name-object pairs were presented for 3500ms each and participants were instructed to think of the person interacting with the object during the entire duration, as it would aid in later memory for that pair. Participants then rated the vividness of their mental image formed on a 1 to 4 scale (strong, moderate, weak, no image) on a new screen that appeared for 1000ms before the new trial began. The retrieval run immediately followed encoding, consisting of 36 name-object pairs. Following a fixation, participants saw a previously studied name (cue) for 1000ms. Next, an object (probe) appeared beneath the name for 2000ms, and participants made a memory response via button press (same, similar, or different image as what was previously paired with the name; or response of “do not know” to avoid guessing). All encoding and retrieval trials were included in analyses. Accuracy was calculated as the percentage of correct responses out of total number of trials.

Statistical Analysis

The evoked responses were analyzed using FSL FEAT^{68,69}. FLAME 1 was used for group-level analysis⁷⁰. After the volumetric data were warped from individual EPI space onto the cortical surface of the template brain, statistical significance of the group-averaged values was calculated by general linear model (GLM) using the Freesurfer command ‘mri_glmfit’, controlling for sex. Correcting for multiple comparisons was performed by Monte Carlo Simulation in FreeSurfer. The number of permutations was set to 4000. The vertex-wise (two-tailed) and cluster-wise (one-tailed) p-value thresholds were 0.05. The corrected p-values were converted back to z scores for visualization.

Layer-dependent Functional Connectivity Analysis

To perform the seed-based FC, we defined the hippocampal seeds based on the group-level statistical maps of hippocampal activation ($p < 0.05$; corrected by FLAME 1). The activation maps of encoding and retrieval were united and the largest two clusters were selected as the hippocampal seeds. The seed time course was obtained by spatially averaging the time courses within each of the hippocampal subregions. The cortico-hippocampal FC was calculated using Pearson correlation coefficient between hippocampal seed and cortical vertex. Cortical regions of interest (ROIs) were similarly defined by merging the activation maps of encoding and retrieval and then selecting the largest activation cluster in visual, dorsal attention, frontoparietal, and default-mode networks. The identified ROIs included visual cortex (VC), posterior parietal cortex (pPC), dorsal lateral prefrontal cortex (dlPFC), and medial prefrontal cortex (mPFC).

To calculate the behavioral correlation with the imbalance of cortico-hippocampal FC strengths between deep and superficial layers, we defined the deeper 1/3 of cortical depth as the deep layers and upper 1/3 as the superficial layers. The middle layers were not included in the FC analysis because neuronal correlations in middle layers over long time periods have been reported to be weak²⁵. The statistical significance of layer-dependent cortico-hippocampal FC between hippocampal seed and cortical ROI was calculated based on the within-ROI Fisher’s Z-transformed FCs that were averaged across deep/superficial layers at each ROI vertex. One-sample t-tests were used to test the statistical significance

of the ROI-averaged Fisher's z value. Note that the behavioral correlation is based on the FC strengths instead of signed FC because the polarity of neurovascular couplings in deep and superficial layers might not be aligned²⁷.

Declarations

Data availability

The data that support the findings of this study are available from the corresponding author upon reasonable request.

Author contributions

W.-T.C. developed MR techniques; S.L. and K.G. designed research; W.-T. C., S.L. and M.S.S. performed research, K.H. and P.-T.Y. implemented the denoising function, W.-T.C., S.L. and M.S.S. analyzed data, W.-T.C., S.L., W.L. and K.G. wrote the paper.

Competing interests

All the authors declare no competing interests.

Acknowledgements

We thank Dr. Feng-Chang Lin for providing helpful opinions on the statistics. This work was supported in part by NIH grants R21AG060324.

References

1. Eichenbaum, H. Prefrontal–hippocampal interactions in episodic memory. *Nat. Rev. Neurosci.* **18**, 547–558 (2017).
2. Mayes, A. R. *et al.* Associative recognition in a patient with selective hippocampal lesions and relatively normal item recognition. *Hippocampus* **14**, 763–784 (2004).
3. Sperling, R. *et al.* Putting names to faces: *NeuroImage* **20**, 1400–1410 (2003).
4. Kim, H. Neural activity that predicts subsequent memory and forgetting: A meta-analysis of 74 fMRI studies. *NeuroImage* **54**, 2446–2461 (2011).
5. Giovanello, K. S. & Dew, I. T. Z. Relational Memory and its Relevance to Aging. in *The Wiley Handbook on the Cognitive Neuroscience of Memory* (eds. Addis, D. R., Barense, M. & Duarte, A.) 371–392 (John Wiley & Sons, Ltd, 2015). doi:10.1002/9781118332634.ch18.

6. Dickerson, B. C. & Eichenbaum, H. The Episodic Memory System: Neurocircuitry and Disorders. *Neuropsychopharmacology* **35**, 86–104 (2010).
7. Squire, L. R. & Zola-Morgan, J. The Cognitive Neuroscience of Human Memory Since H.M. *Annu. Rev. Neurosci.* **34**, 259–288 (2011).
8. Wing, E. A., Ritchey, M. & Cabeza, R. Reinstatement of Individual Past Events Revealed by the Similarity of Distributed Activation Patterns during Encoding and Retrieval. *J. Cogn. Neurosci.* **27**, 679–691 (2015).
9. Kuhl, B. A., Bainbridge, W. A. & Chun, M. M. Neural Reactivation Reveals Mechanisms for Updating Memory. *J. Neurosci.* **32**, 3453–3461 (2012).
10. Uncapher, M. R. & Wagner, A. D. Posterior parietal cortex and episodic encoding: Insights from fMRI subsequent memory effects and dual-attention theory. *Neurobiol. Learn. Mem.* **91**, 139–154 (2009).
11. Grady, C. L., McIntosh, A. R. & Craik, F. I. M. Age-related differences in the functional connectivity of the hippocampus during memory encoding. *Hippocampus* **13**, 572–586 (2003).
12. Menon, V., Boyett-Anderson, J. M. & Reiss, A. L. Maturation of medial temporal lobe response and connectivity during memory encoding. *Cogn. Brain Res.* **25**, 379–385 (2005).
13. Sestieri, C., Corbetta, M., Romani, G. L. & Shulman, G. L. Episodic Memory Retrieval, Parietal Cortex, and the Default Mode Network: Functional and Topographic Analyses. *J. Neurosci.* **31**, 4407–4420 (2011).
14. Shapira-Lichter, I., Oren, N., Jacob, Y., Gruberger, M. & Hendler, T. Portraying the unique contribution of the default mode network to internally driven mnemonic processes. *Proc. Natl. Acad. Sci.* **110**, 4950–4955 (2013).
15. Cooper, R. A. & Ritchey, M. Cortico-hippocampal network connections support the multidimensional quality of episodic memory. *eLife* **8**, e45591 (2019).
16. Westphal, A. J., Wang, S. & Rissman, J. Episodic Memory Retrieval Benefits from a Less Modular Brain Network Organization. *J. Neurosci.* **37**, 3523–3531 (2017).
17. Tang, L. *et al.* Differential Functional Connectivity in Anterior and Posterior Hippocampus Supporting the Development of Memory Formation. *Front. Hum. Neurosci.* **14**, 204 (2020).
18. Hrybouski, S. *et al.* Involvement of hippocampal subfields and anterior-posterior subregions in encoding and retrieval of item, spatial, and associative memories: Longitudinal versus transverse axis. *NeuroImage* **191**, 568–586 (2019).

19. Suthana, N. A. *et al.* High-resolution 7T fMRI of Human Hippocampal Subfields during Associative Learning. *J. Cogn. Neurosci.* **27**, 1194–1206 (2015).
20. Duncan, K., Tompary, A. & Davachi, L. Associative Encoding and Retrieval Are Predicted by Functional Connectivity in Distinct Hippocampal Area CA1 Pathways. *J. Neurosci.* **34**, 11188–11198 (2014).
21. Ven, V. *et al.* Hippocampal-striatal functional connectivity supports processing of temporal expectations from associative memory. *Hippocampus* **30**, 926–937 (2020).
22. Reagh, Z. M., Watabe, J., Ly, M., Murray, E. & Yassa, M. A. Dissociated Signals in Human Dentate Gyrus and CA3 Predict Different Facets of Recognition Memory. *J. Neurosci.* **34**, 13301–13313 (2014).
23. Lacy, J. W., Yassa, M. A., Stark, S. M., Muftuler, L. T. & Stark, C. E. Distinct pattern separation related transfer functions in human CA3/dentate and CA1 revealed using high-resolution fMRI and variable mnemonic similarity. *Learn Mem* **18**, 15–8 (2011).
24. Buffalo, E. A., Fries, P., Landman, R., Buschman, T. J. & Desimone, R. Laminar differences in gamma and alpha coherence in the ventral stream. *Proc. Natl. Acad. Sci.* **108**, 11262–11267 (2011).
25. Smith, M. A., Jia, X., Zandvakili, A. & Kohn, A. Laminar dependence of neuronal correlations in visual cortex. *J. Neurophysiol.* **109**, 940–947 (2013).
26. Maier. Distinct Superficial and deep laminar domains of activity in the visual cortex during rest and stimulation. *Front. Syst. Neurosci.* (2010) doi:10.3389/fnsys.2010.00031.
27. Scheeringa, R., Koopmans, P. J., van Mourik, T., Jensen, O. & Norris, D. G. The relationship between oscillatory EEG activity and the laminar-specific BOLD signal. *Proc Natl Acad Sci U A* **113**, 6761–6 (2016).
28. Fischl, B. & Dale, A. M. Measuring the thickness of the human cerebral cortex from magnetic resonance images. *Proc. Natl. Acad. Sci.* **97**, 11050–11055 (2000).
29. Griffiths, B. J. *et al.* Directional coupling of slow and fast hippocampal gamma with neocortical alpha/beta oscillations in human episodic memory. *Proc Natl Acad Sci U A* **116**, 21834–21842 (2019).
30. Axmacher, N. *et al.* Cross-frequency coupling supports multi-item working memory in the human hippocampus. *Proc. Natl. Acad. Sci.* **107**, 3228–3233 (2010).
31. Dalton, M. A., McCormick, C. & Maguire, E. A. Differences in functional connectivity along the anterior-posterior axis of human hippocampal subfields. *NeuroImage* **192**, 38–51 (2019).
32. T. Vu, A. *et al.* Tradeoffs in pushing the spatial resolution of fMRI for the 7T Human Connectome Project. *NeuroImage* **154**, 23–32 (2017).

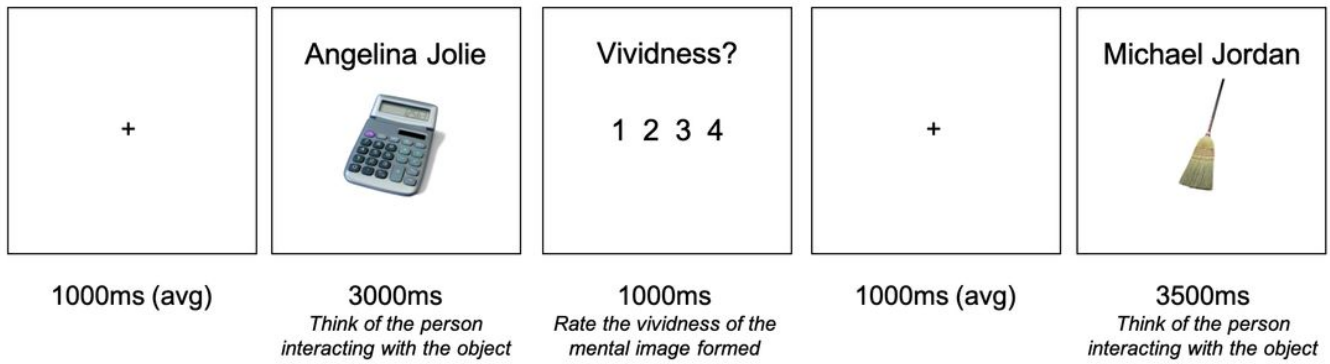
33. Setsompop, K. *et al.* Blipped-controlled aliasing in parallel imaging for simultaneous multislice echo planar imaging with reduced *g*-factor penalty: Blipped-CAIPI for Simultaneous Multislice EPI. *Magn. Reson. Med.* **67**, 1210–1224 (2012).
34. Veraart, J., Fieremans, E. & Novikov, D. S. Diffusion MRI noise mapping using random matrix theory. *Magn Reson Med* **76**, 1582–1593 (2016).
35. Chai, X. J., Ofen, N., Gabrieli, J. D. E. & Whitfield-Gabrieli, S. Development of deactivation of the default-mode network during episodic memory formation. *NeuroImage* **84**, 932–938 (2014).
36. Huijbers, W., Pennartz, C. M. A., Cabeza, R. & Daselaar, S. M. The Hippocampus Is Coupled with the Default Network during Memory Retrieval but Not during Memory Encoding. *PLoS ONE* **6**, e17463 (2011).
37. Morris, C. D., Bransford, J. D. & Franks, J. J. Levels of processing versus transfer appropriate processing. *J. Verbal Learn. Verbal Behav.* **16**, 519–533 (1977).
38. Yassa, M. A. & Stark, C. E. L. Pattern separation in the hippocampus. *Trends Neurosci.* **34**, 515–525 (2011).
39. Neunuebel, J. P. & Knierim, J. J. CA3 Retrieves Coherent Representations from Degraded Input: Direct Evidence for CA3 Pattern Completion and Dentate Gyrus Pattern Separation. *Neuron* **81**, 416–427 (2014).
40. Vogt, B. A. & Miller, M. W. Cortical connections between rat cingulate cortex and visual, motor, and postsubicular cortices. *J. Comp. Neurol.* **216**, 192–210 (1983).
41. Wang, L., Saalman, Y. B., Pinski, M. A., Arcaro, M. J. & Kastner, S. Electrophysiological Low-Frequency Coherence and Cross-Frequency Coupling Contribute to BOLD Connectivity. *Neuron* **76**, 1010–1020 (2012).
42. Goense, J. B. M. & Logothetis, N. K. Neurophysiology of the BOLD fMRI Signal in Awake Monkeys. *Curr. Biol.* **18**, 631–640 (2008).
43. Bone, M. B., Ahmad, F. & Buchsbaum, B. R. Feature-specific neural reactivation during episodic memory. *Nat. Commun.* **11**, 1945 (2020).
44. Nyhus, E. & Curran, T. Functional role of gamma and theta oscillations in episodic memory. *Neurosci. Biobehav. Rev.* **34**, 1023–1035 (2010).
45. Lisman, J. E. & Jensen, O. The Theta-Gamma Neural Code. *Neuron* **77**, 1002–1016 (2013).
46. Bastos, A. M., Loonis, R., Kornblith, S., Lundqvist, M. & Miller, E. K. Laminar recordings in frontal cortex suggest distinct layers for maintenance and control of working memory. *Proc. Natl. Acad. Sci.* **115**, 1117–1122 (2018).

47. Lachaux, J. P. *et al.* Relationship between task-related gamma oscillations and BOLD signal: new insights from combined fMRI and intracranial EEG. *Hum Brain Mapp* **28**, 1368–75 (2007).
48. Koch, S. P., Werner, P., Steinbrink, J., Fries, P. & Obrig, H. Stimulus-Induced and State-Dependent Sustained Gamma Activity Is Tightly Coupled to the Hemodynamic Response in Humans. *J. Neurosci.* **29**, 13962–13970 (2009).
49. Buxton, R. B., Uludag, K., Dubowitz, D. J. & Liu, T. T. Modeling the hemodynamic response to brain activation. *Neuroimage* **23 Suppl 1**, S220-33 (2004).
50. Scheeringa, R. *et al.* Neuronal Dynamics Underlying High- and Low-Frequency EEG Oscillations Contribute Independently to the Human BOLD Signal. *Neuron* **69**, 572–583 (2011).
51. Khursheed, F. *et al.* Frequency-specific electrocorticographic correlates of working memory delay period fMRI activity. *NeuroImage* **56**, 1773–1782 (2011).
52. Qin, Q. Point spread functions of the T2 decay in k-space trajectories with long echo train. *Magn. Reson. Imaging* **30**, 1134–1142 (2012).
53. Peters, A. M. *et al.* T2* measurements in human brain at 1.5, 3 and 7 T. *Magn. Reson. Imaging* **25**, 748–753 (2007).
54. Petridou, N. & Siero, J. C. W. Laminar fMRI: What can the time domain tell us? *NeuroImage* **197**, 761–771 (2019).
55. Huber, L. R. *et al.* LayNii: A software suite for layer-fMRI. *Neuroimage* **237**, 118091 (2021).
56. Leparulo, A. *et al.* Accelerated Aging Characterizes the Early Stage of Alzheimer's Disease. *Cells* **11**, 238 (2022).
57. Goutagny, R. *et al.* Alterations in hippocampal network oscillations and theta-gamma coupling arise before Abeta overproduction in a mouse model of Alzheimer's disease. *Eur J Neurosci* **37**, 1896–902 (2013).
58. Blum, S., Habeck, C., Steffener, J., Razlighi, Q. & Stern, Y. Functional connectivity of the posterior hippocampus is more dominant as we age. *Cogn. Neurosci.* **5**, 150–159 (2014).
59. Salami, A., Pudas, S. & Nyberg, L. Elevated hippocampal resting-state connectivity underlies deficient neurocognitive function in aging. *Proc. Natl. Acad. Sci.* **111**, 17654–17659 (2014).
60. Buzsáki, G. & Draguhn, A. Neuronal Oscillations in Cortical Networks. *Science* **304**, 1926–1929 (2004).
61. Hangya, B., Borhegyi, Z., Szilagyi, N., Freund, T. F. & Varga, V. GABAergic Neurons of the Medial Septum Lead the Hippocampal Network during Theta Activity. *J. Neurosci.* **29**, 8094–8102 (2009).

62. Griswold, M. A. *et al.* Generalized autocalibrating partially parallel acquisitions (GRAPPA). *Magn Reson Med* **47**, 1202–10 (2002).
63. Smith, S. M. *et al.* Advances in functional and structural MR image analysis and implementation as FSL. *Neuroimage* **23 Suppl 1**, S208-19 (2004).
64. Beckmann, C. F., DeLuca, M., Devlin, J. T. & Smith, S. M. Investigations into resting-state connectivity using independent component analysis. *Philos. Trans. R. Soc. Lond. B. Biol. Sci.* **360**, 1001–1013 (2005).
65. Salimi-Khorshidi, G. *et al.* Automatic denoising of functional MRI data: combining independent component analysis and hierarchical fusion of classifiers. *Neuroimage* **90**, 449–68 (2014).
66. Stark, S. M., Kirwan, C. B. & Stark, C. E. L. Mnemonic Similarity Task: A Tool for Assessing Hippocampal Integrity. *Trends Cogn. Sci.* **23**, 938–951 (2019).
67. Dale, A. M. Optimal experimental design for event-related fMRI. *Hum. Brain Mapp.* **8**, 109–114 (1999).
68. Woolrich, M. W., Ripley, B. D., Brady, M. & Smith, S. M. Temporal autocorrelation in univariate linear modeling of FMRI data. *NeuroImage* **14**, 1370–1386 (2001).
69. Woolrich, M. W., Behrens, T. E. J. & Smith, S. M. Constrained linear basis sets for HRF modelling using Variational Bayes. *NeuroImage* **21**, 1748–1761 (2004).
70. Woolrich, M. W., Behrens, T. E. J., Beckmann, C. F., Jenkinson, M. & Smith, S. M. Multilevel linear modelling for FMRI group analysis using Bayesian inference. *NeuroImage* **21**, 1732–1747 (2004).

Figures

A. Encoding



B. Retrieval

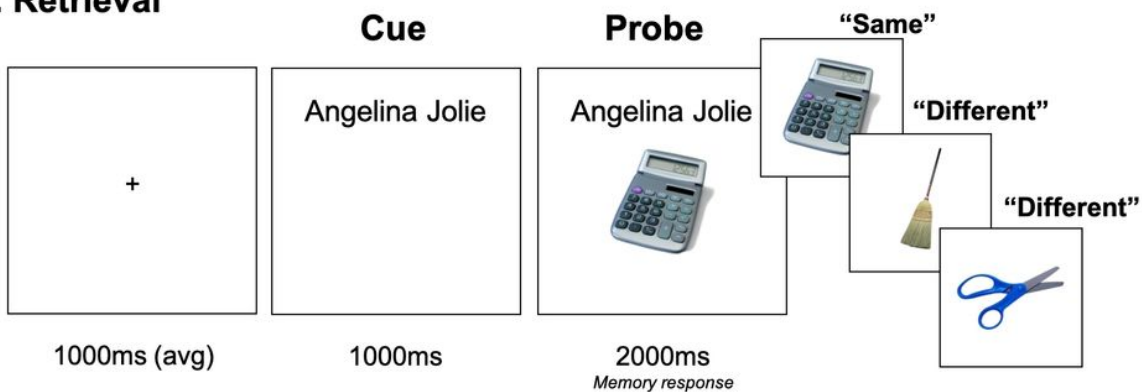


Figure 1

Task Paradigm. (A) Encoding phase: Participants study pairs of names of famous figures and pictures of everyday objects, then rate the vividness of the mental image they were able to form via button box press. (B) Retrieval phase: A name from the study phase appears as a cue for 1000ms, then an image appears below the name. At this time, the participant indicates via button box press whether the image is the same as, similar to, or different from the image previously paired with the name.

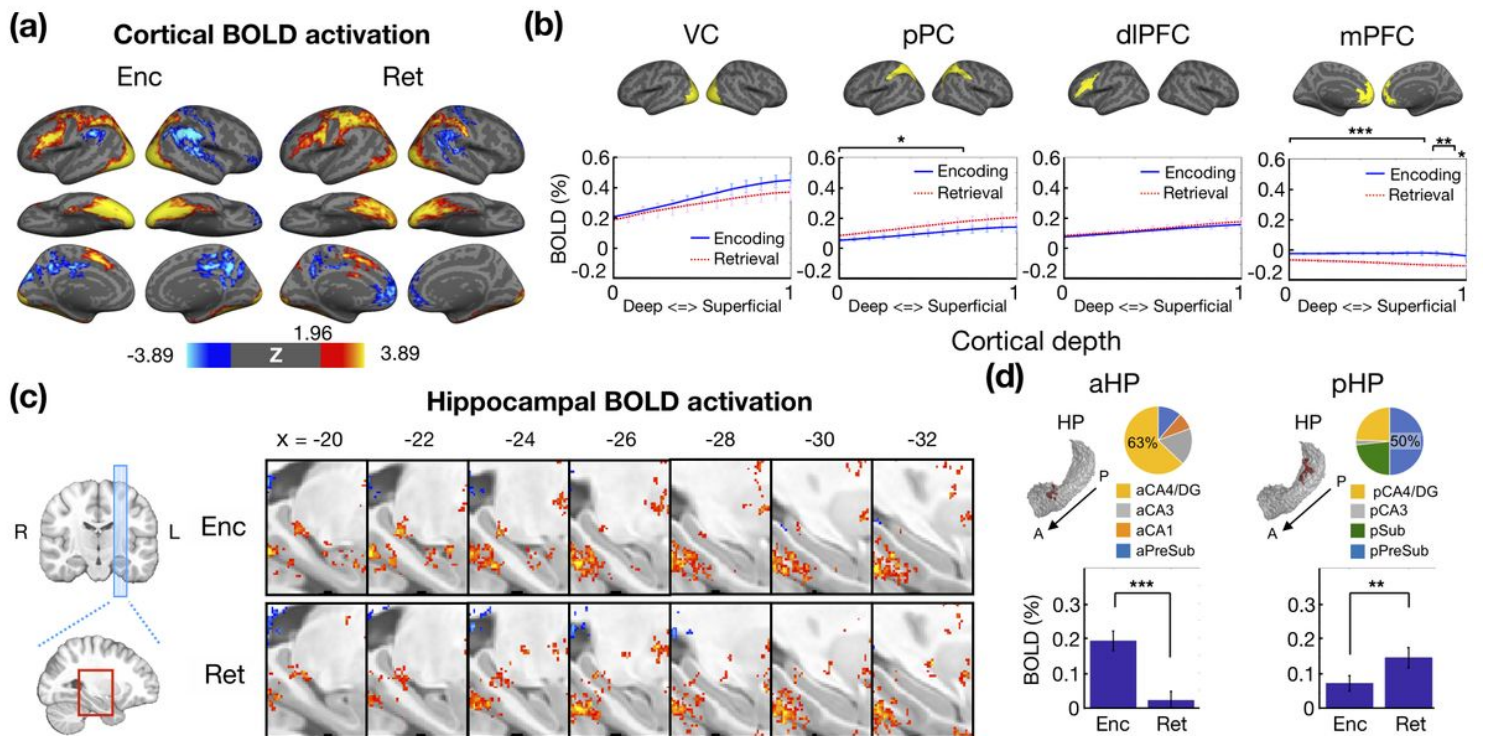


Figure 2

Cortical and hippocampal activations during memory encoding and retrieval. (a) The statistical maps of BOLD activation during encoding and retrieval are shown on the left and right panels respectively ($p < 0.05$; corrected by Monte Carlo simulation test). The z scores are encoded as indicated by the color bar. (b) The cortical-depth profiles of averaged BOLD signal changes in different ROIs. The blue solid traces and red dotted traces represent the percentage of BOLD signal changes during encoding and retrieval respectively. The error bar represents the standard error of mean (SEM). The 0 on the x axis represents the grey-white matter boundary, and 1 represents the white matter-CSF boundary. (c) The statistical maps of BOLD activation in the proximity of hippocampus ($p < 0.05$; corrected by FSL FLAME 1). The left most column illustrates the location of sagittal slices and the red box indicates the region of the zoom-in views. The x values in the right panel are of MNI coordinates. (d) The hippocampal activation clusters as highlighted in dark red are defined by the evoked BOLD activations. The pie charts illustrate the composition of the clusters with respect to the hippocampal subfields. The percentages of BOLD signal changes within each cluster are shown in the bar charts. The error bars indicate the SEM. The asterisks indicate the level of statistical significance by t-test. *: $p < 0.05$; **: $p < 0.01$; ***: $p < 0.001$. Abbreviations: Enc – encoding; Ret – retrieval; VC - visual cortex; pPC – posterior parietal cortex; dlPFC - dorsal lateral prefrontal cortex; mPFC - medial prefrontal cortex; R – Right; L – Left; a – anterior; p – posterior; HP – hippocampus; CA - Cornu Ammonis; DG – dentate gyrus; Sub – subiculum; PreSub – presubiculum.

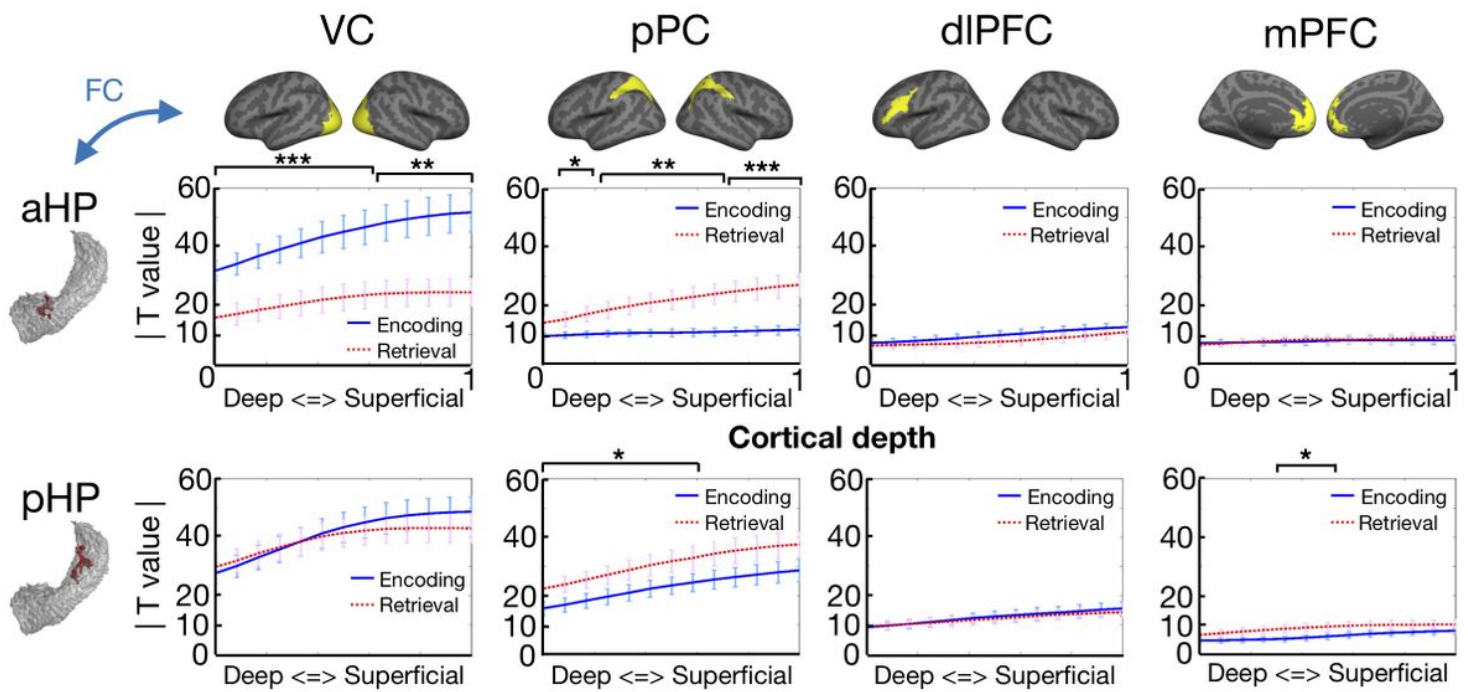


Figure 3

Cortical-depth profiles of cortico-hippocampal FC associated with different cortical ROIs. The upper and lower rows are associated with aHP and pHP respectively. The blue solid traces and red dotted traces represent the cortico-hippocampal FC during encoding and retrieval stages, respectively. The asterisks indicate the statistical significance of between-stage differences using t-test. *: $p < 0.05$; **: $p < 0.01$; ***: $p < 0.001$. The error bars represent the SEM. Abbreviations: Enc – encoding; Ret – retrieval; VC - visual cortex; pPC – posterior parietal cortex; dIPFC - dorsal lateral prefrontal cortex; mPFC - medial prefrontal cortex

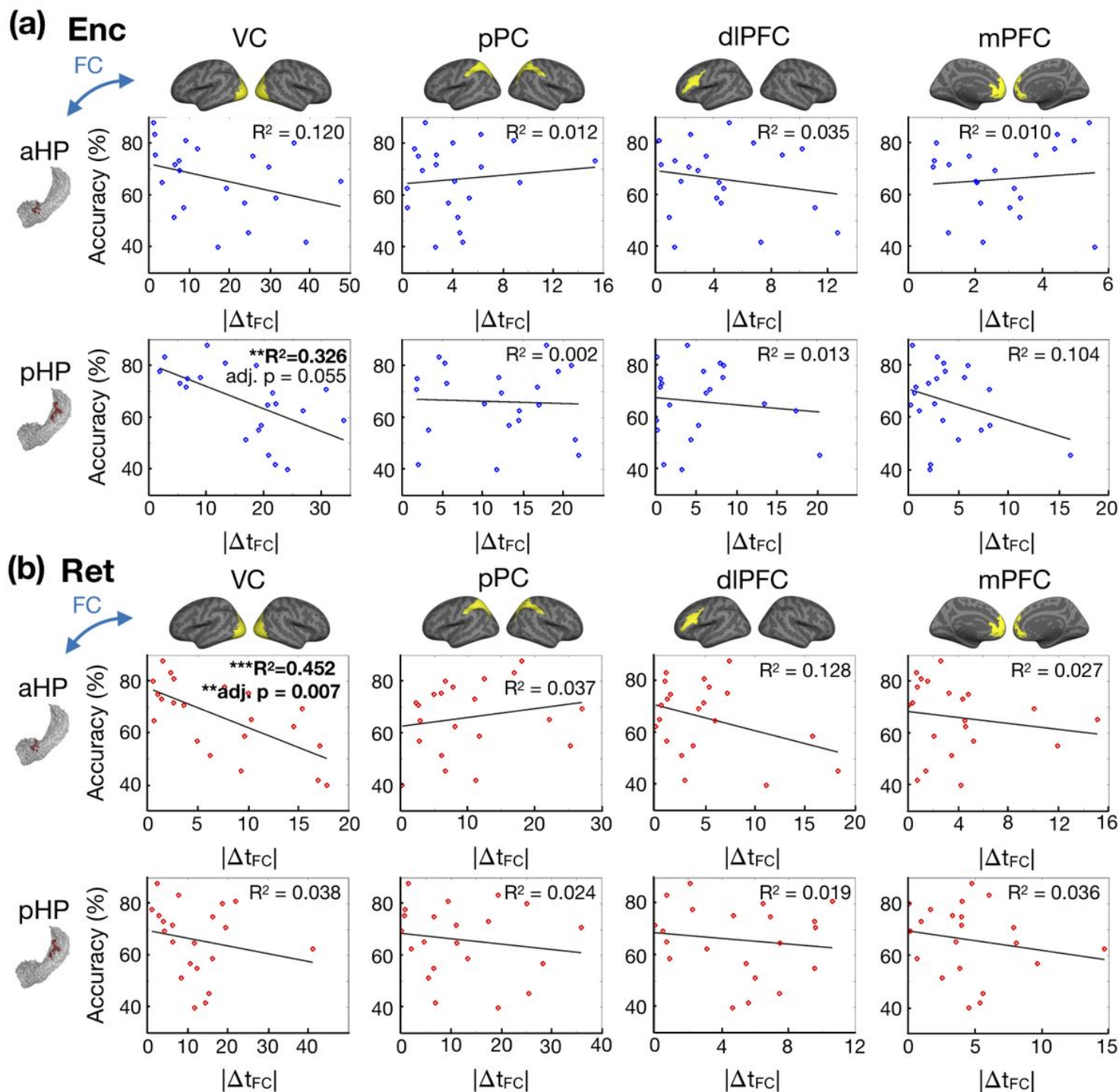


Figure 4

Behavioral correlations with cross-layer imbalance of cortico-hippocampal FC. (a) The behavioral correlations during encoding stage. (b) The behavioral correlations during retrieval stage. In each panel, the x axis represents the difference of cortico-hippocampal FC strengths between deep and superficial layers. $\Delta t_{FC} = |t_{FC,deep}| - |t_{FC,sup}|$ where $t_{FC,deep}$ and $t_{FC,sup}$ indicate the t values of FC associated with deep and superficial layers respectively. The y axis represents the in-scanner accuracy of memory retrieval. The blue and red circles represent the individual data points in encoding and retrieval stages respectively. The

boldface values indicate statistical significance at $p < 0.05$. The asterisks indicate the statistical significance. **: $p < 0.01$; ***: $p < 0.001$.

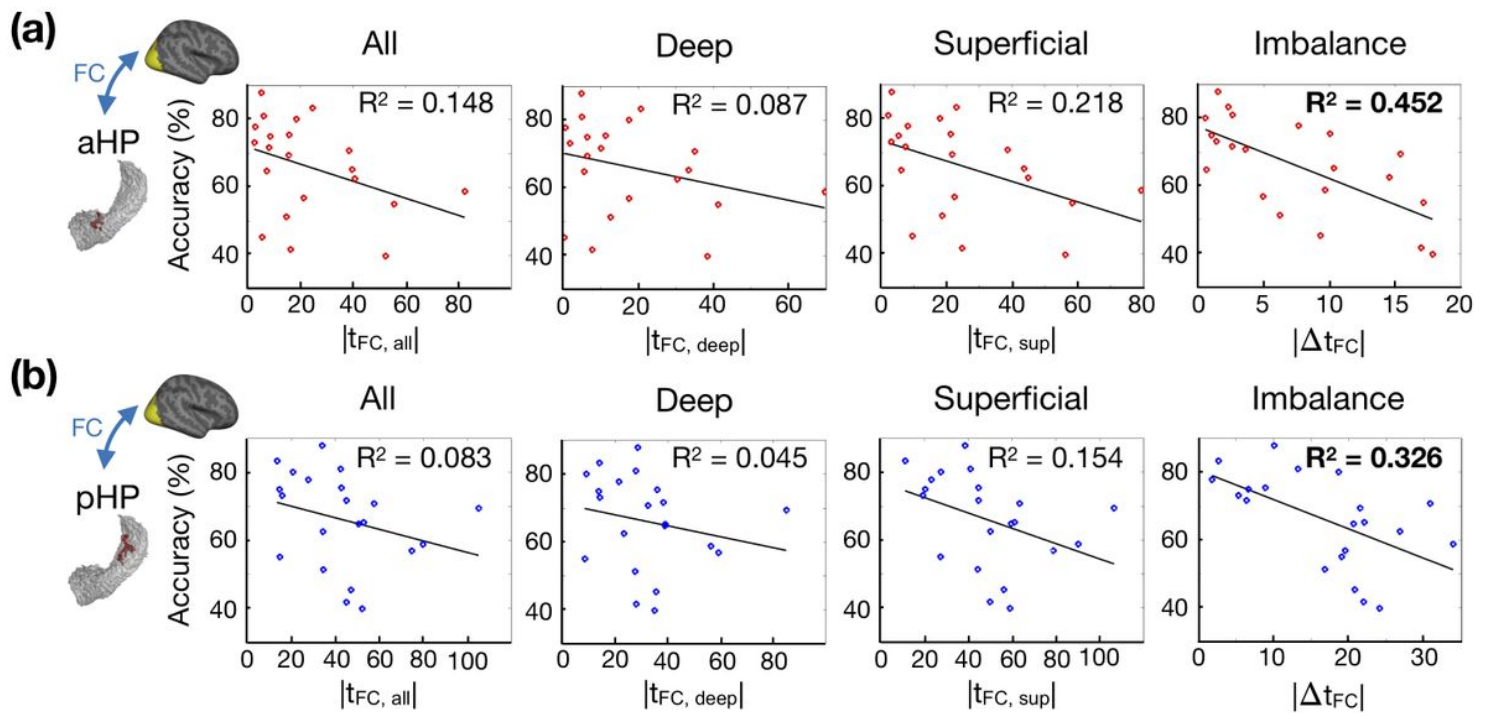


Figure 5

Behavioral correlations with different types of cortico-hippocampal FCs during (a) retrieval and (b) encoding stages. $t_{FC,all}$, $t_{FC,deep}$, $t_{FC,sup}$ indicate the t values of FC associated with all, deep and superficial layers respectively. $\Delta t_{FC} = |t_{FC,deep}| - |t_{FC,sup}|$. The cross-layer imbalance of cortico-hippocampal FC $|\Delta t_{FC}|$ is a better predictor of recognition accuracy than all the other types of FC ($p < 0.001$ using bootstrapping) in both encoding and retrieval stages.

Supplementary Files

This is a list of supplementary files associated with this preprint. Click to download.

- [laminarhipposupplefinal.docx](#)